KRONOS FUSION ENERGY

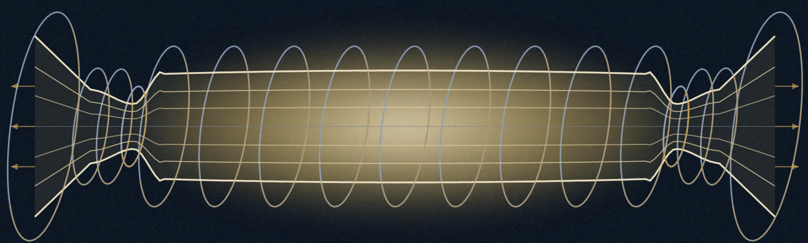

PAPER II OF THE 2026 KRONOS SET

Aegis & MetroVolt

The Generator

A deuterium–helium-3 tandem-mirror generator that closes on measured efficiencies — two housings, one machine.

Tandem mirror · $D–^3He$ · Q_E 1.31 · f_n 5.44% · +104 / 850 / 2832 MW_e

Explore it live — 3-D model · physics validator · film series

PREPARED BY P. I. FORD · G. L. KULCINSKI

2026 · EDITORIAL

KRONOS FUSION ENERGY · 2026

The Kronos Fleet

Fuel follows purpose, not platform.

Hyperion · Aegis · MetroVolt

THE OFFICIAL RECORD

What this document is, and how to read its numbers

This is a combined editorial. It gathers, in one volume, the two design studies Kronos Fusion Energy released in 2026 — a compact spherical-tokamak tritium/helium-3 breeder and a deuterium–helium-3 tandem-mirror generator — together with the intellectual-property estate, the people, and, in the internal edition, the full commercial case. The scientific text is the same text that appears in the arXiv preprints and the journal submissions; the editorial adds the apparatus a reader needs to hold the whole program at once, and nothing in the physics is altered to fit it.

THE HONESTY STANCE IS THE ASSET

Every headline quantity carries an **evidence class** — DERIVED RECOMPUTED MEASURED REQUIREMENT — and, where a number is a modelled extrapolation rather than a demonstrated value, it is labelled as such and its downside is shown next to it. Several quantities in the underlying corpus moved after first publication; where a value has been withdrawn or restated, the record says so plainly. This is deliberate: a diligence team will find the load-bearing assumptions, so the document surfaces them first.

TITLE	The Kronos Fleet — Hyperion · Aegis · MetroVolt: A Combined Design & Commercialization Study
AUTHOR	Priyanca Ford, Founder & CEO, on behalf of Kronos Fusion Energy
EDITION	2026 Combined Editorial · first issue
COMPANION WORKS	The five-paper arXiv drop — (1) Breeder, (2) Burner, (3) REBCO magnet & tape, (4) Direct Energy Conversion, (5) AI/ML/Quantum control — with matching numbered Zenodo deposits, plus the IOP journal and IAEA-FEC submissions. Patents were filed before the drop.
NAMING	Hyperion = the breeder; Aegis (defense) and MetroVolt (data-center) = one generator in two housings. Internal mode letters (D1, L) do not appear on public surfaces.
STATUS	Conceptual design & simulation study. Nothing herein is a construction commitment.

HOW TO READ THIS VOLUME

The fleet at a glance, and the way its numbers are marked

This volume opens with *Orientation*, presents the five research papers as a bound sequence, and closes with the *Apparatus*. *Foundations* sets out the three general results both machines rest on. *Paper One* is the Hyperion breeder; *Paper Two* the Aegis / MetroVolt generator; *Papers Three, Four and Five* are the enabling science — high-field REBCO magnets and tape, direct energy conversion, and the AI / ML / quantum control stack. A *Digital Twin & 3-D Model* part follows, then the *Environmental* profile. The *Economics* and levelized cost and the *Business Case* and diligence record appear in the internal edition only; the *Simulations* proof record and the Apparatus — patent portfolio, team, limitations, and sources — close both editions.

THE FLEET AT A GLANCE

	HYPERION	AEGIS	METROVOLT
Role	Strategic-isotope foundry	Defense installation power	Campus power
Machine	**Spherical tokamak**	**Tandem mirror**	**Tandem mirror**
Fuel	Deuterium–tritium	Deuterium–helium-3	Deuterium–helium-3
Delivers	Tritium · ^{3}He · 14 MeV n	Resilient installation power	Firm campus power
Physics bar	**Fusion gain only**	Closure (gates named)	Closure + lunar ^{3}He
In the fleet	Breeds the fuel	Proves the generator	Commercial destination

HOW THE NUMBERS ARE MARKED

Every headline quantity carries an evidence class — DERIVED from first principles, RECOMPUTED from raw data, MEASURED in hardware, or a REQUIREMENT yet to be met. Financial figures carry a case label and are confined to the internal (confidential) edition. Values that moved after first publication are shown as withdrawn or restated rather than quietly changed. A capability you can evaluate is one whose limits are on the page.

ABSTRACT

Aegis & MetroVolt — The Generator

Aegis and MetroVolt are two application housings of one deuterium–helium-3 tandem mirror that closes on *measured* component efficiencies. Its principal new result: synchrotron reabsorption is not a fixed fraction of fusion power but scales with machine size, an analytic consequence of a harmonic cutoff that grows as the one-third power of minor radius. At the Mode M closing point the engineering gain is Q_E 1.31 at a low neutron fraction of 5.44% — low-neutron, never aneutronic. Closure is requirement-class, not demonstrated: it needs an end-plug density ratio of 16 (347× the GDT-measured value), stated as the design's largest open item.

Companion deposit (code & data, reproducible under CC BY 4.0): DOI 10.5281/zenodo.21746479 · Zenodo community *kronos_fusion_energy*.
Explore it live: interactive 3-D model · run the physics validator · companion film series (the deposited solvers, in the browser).

Keywords: tandem mirror · deuterium–helium-3 · direct energy conversion · synchrotron reabsorption · low-neutron

CONTENTS

Table of Contents

PORTFOLIO, PEOPLE & RECORD

NOMENCLATURE

Symbols, units, and the names of things

Q	plasma (fusion) gain, P_{fus}/P_{aux}
Q_E	engineering gain, net electric out / recirculating in
H_{98}	confinement enhancement over the IPB98(y,2) scaling
Z_{eff}	effective ion charge
c_{ee}	electron–electron bremsstrahlung leading coefficient, 2.120022 (exact)
τ_E	energy confinement time
I_p	plasma current
R_0, a	major radius, minor radius
κ, δ	elongation, triangularity
β_N	normalized plasma beta (Troyon-normalized)
TBR	tritium breeding ratio
DEC	direct energy conversion
CF	plant capacity factor (availability)
FOAK / NOAK / BOAK	first / n^{th} / best of a kind
Hyperion	the ST breeder (internal: Mode D2)
Aegis	the generator, defense/installation housing (internal: Mode M)
MetroVolt	the generator, data-center housing (Mode M)

§ 1

Why a mirror, and what this paper actually claims

A deuterium–helium-3 fusion generator is attractive for exactly the reason it is hard: most of its energy emerges as *charged* particles that can, in principle, be converted to electricity directly — without a steam cycle, and at low neutron output. Capturing that advantage requires *open* magnetic field lines, so that the charged exhaust can be steered into a direct energy converter. That rules out the tokamak and points to a mirror. The tandem mirror with a high-field end plug is the natural configuration, and it carries a long design lineage: *Ra*, the D–^{3}He axisymmetric tandem mirror with Venetian-blind direct conversion; the ARTEMIS D–^{3}He field-reversed-configuration plant of Momota and colleagues; and the recent high-field HTS mirror hardware demonstrated on WHAM.

This paper does not claim a new mirror concept. It does three things a design study of this class should do and rarely does. First, it **closes the power balance on *measured* component efficiencies** and reports the result with the model's own numerical-validity flag attached, rather than on an aspirational converter efficiency. Second, it contributes one genuinely new physics result — that the **synchrotron effective harmonic cutoff scales with machine size**, $n^* \propto a^{1/3}$, so that synchrotron loss is a design lever, not a fixed fraction of fusion power. Third, it **names its extrapolations** rather than absorbing them into a single blended optimum: two are retired to "engineering, not physics," and exactly one — the thermal barrier — remains a genuine physics gate with a measured historical negative.

READ EVERY GAIN NUMBER WITH THIS CAVEAT ATTACHED

The generator closes with positive engineering gain at its design operating point — Q_E = 1.31 — but that closure is **requirement-class, not demonstrated**. It depends on an end-plug density ratio $n_p/n_c \approx 16$, a plug density of $\approx 4\times10^{21}\ \mathrm{m}^{-3}$ that is **347× the best value ever measured on a tandem-mirror plug** (GDT), and roughly two orders of magnitude above any operated device. It is the design's single largest open item. At the reference ratio $n_p/n_c = 10$ the balance does *not* close (Q_E = 0.63). Every Q_E in this paper is quoted only with this requirement attached, and the fuel is described throughout as **low-neutron, never aneutronic** (f_n = 5.44% at the design point). REQUIREMENT-CLASS

Economics are reported in a separate companion and are not a condition of any result here. The physics stands on its own; the technology base — high-field magnets and direct conversion — is the near-term value.

§ 2

Methods — how the balance is evaluated, and where the flags live

The central-cell power balance is evaluated with charged-particle, bremsstrahlung and synchrotron channels resolved separately. Bremsstrahlung uses a relativistic form with the *exact* electron–electron coefficient

$$c_{ee} = 5(44 - 3\pi^2) / (24\sqrt{2}) = 2.120022 \quad (1)$$

rather than the widely circulated 1.499 (the same expression with √2 replaced by 2). Synchrotron reabsorption is treated with an effective harmonic cutoff (§7) whose reabsorption model reproduces a published tokamak loss to within a factor of order unity — in contrast to optically-thin forms that over-predict by three orders of magnitude at reactor conditions. DERIVED · EXACT

Direct-conversion efficiencies are taken from the measured tube record where one exists, and are otherwise flagged as requirements; the per-stage values and their sources are set out in §8. **The plug field** is computed self-consistently from the Frank relation

$$\varphi_i = T_e \ln(n_p/n_c) \quad (2)$$

which couples the plug drive power to the confining potential, evaluated at the density ratio $n_p/n_c \approx 16$ that closure requires; the throat field is therefore reported as a *pair* (ion end, thermal end) rather than a single number. **Closure** is reported at the design operating point $x(^3He) = 0.30$, where Q_E exceeds unity across $x(^3He) \in [0.20, 0.43]$ at the required plug ratio, and the operating point passes the solver's own near-ignition guard (`near_ignition = False`). The discipline throughout is that a measured value and a required value are never averaged into a single optimum — they are carried on separate ledgers so that a diligence reader can see which is which. RECOMPUTED

§ 3

The shared result the converter analysis rests on

Four general results of the companion breeder study — the self-heating knife edge, gain saturation under unbounded confinement, the affine effective-charge scaling, and the distinction between charged and directable power — apply here unchanged. The last is *load-bearing* for the direct-conversion analysis, and it is worth stating in its own right, because it governs what a converter can and cannot capture.

A charged fusion product is locally depositing; it is not thereby **directable**. A three-body final state yields a *continuum* rather than discrete lines, and a continuum cannot be efficiency-matched to an electrostatic converter the way two discrete lines can. The D–^{3}He proton and alpha are two discrete lines — favourable for grid-stack conversion. A ^{3}He–^{3}He reaction, by contrast, produces a three-body continuum that carries *no* transferable conversion efficiency. Any converter efficiency quoted across two fuels of different final-state multiplicity is wrong on its face; this is a definitional constraint, not a modelling choice, and it is why the ledger of §8 never credits the ^{3}He–^{3}He channel with the D–^{3}He tube number. DERIVED · DEFINITIONAL

§ 4

The device — an axisymmetric high-field tandem mirror

The generator is an axisymmetric high-field tandem mirror with end plugs and direct energy conversion on the open field lines. A straight central cell — where the D–^{3}He fuel burns — is closed at each end by a mirror throat and a high-field plug that raises the confining electrostatic potential; the axial loss that leaks past the plugs is not wasted but steered into the direct-conversion end tanks. The three figures below give the machine at a glance: the axial layout, the central-cell cross-section, and the axial field profile from the central cell through the mirror throat to the plug.

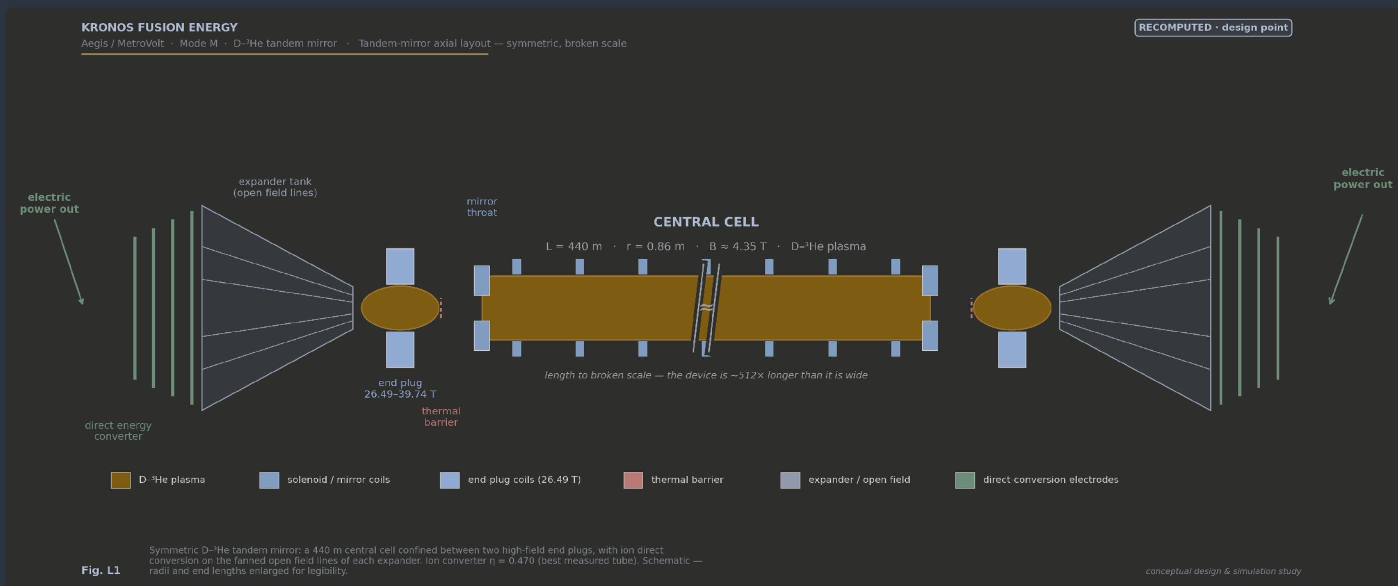

FIGURE 1. Tandem-mirror axial layout: central cell, mirror throats, end plugs, and the direct-conversion end tanks (conceptual design; no machine has been built). RECOMPUTED

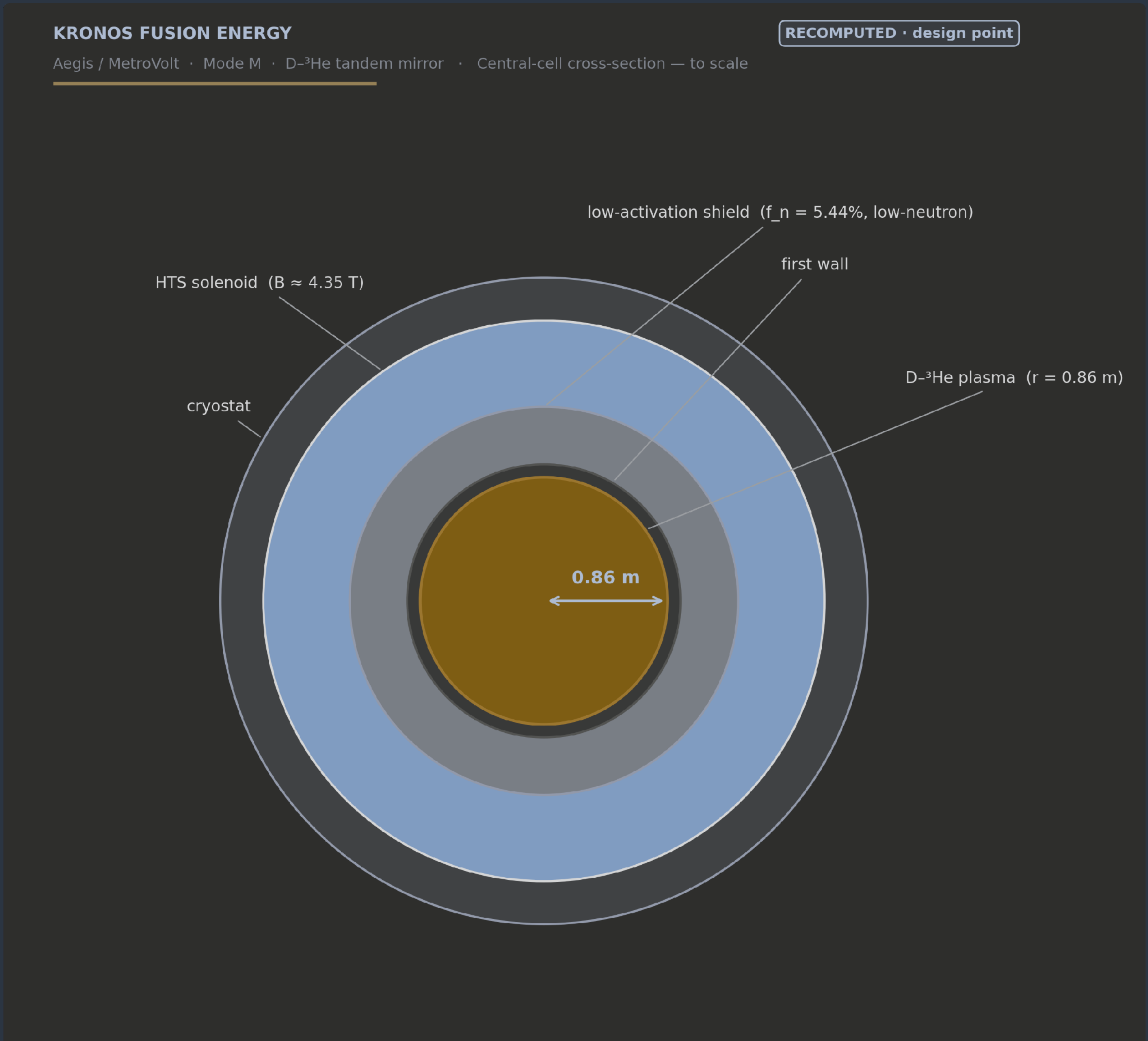

Fig. L2 Axisymmetric central cell: a simply-connected circular plasma with no toroidal field coils. D–^{3}He at f_n = 5.44% is low-neutron (never aneutronic), permitting a thin low-activation shield rather than a breeding blanket.

conceptual design & simulation study

FIGURE 2. Central-cell cross-section — the circular D–^{3}He plasma at minor radius a = 0.86 m, its shield, the HTS central-cell solenoid at 4.35 T, and the cryostat. RECOMPUTED

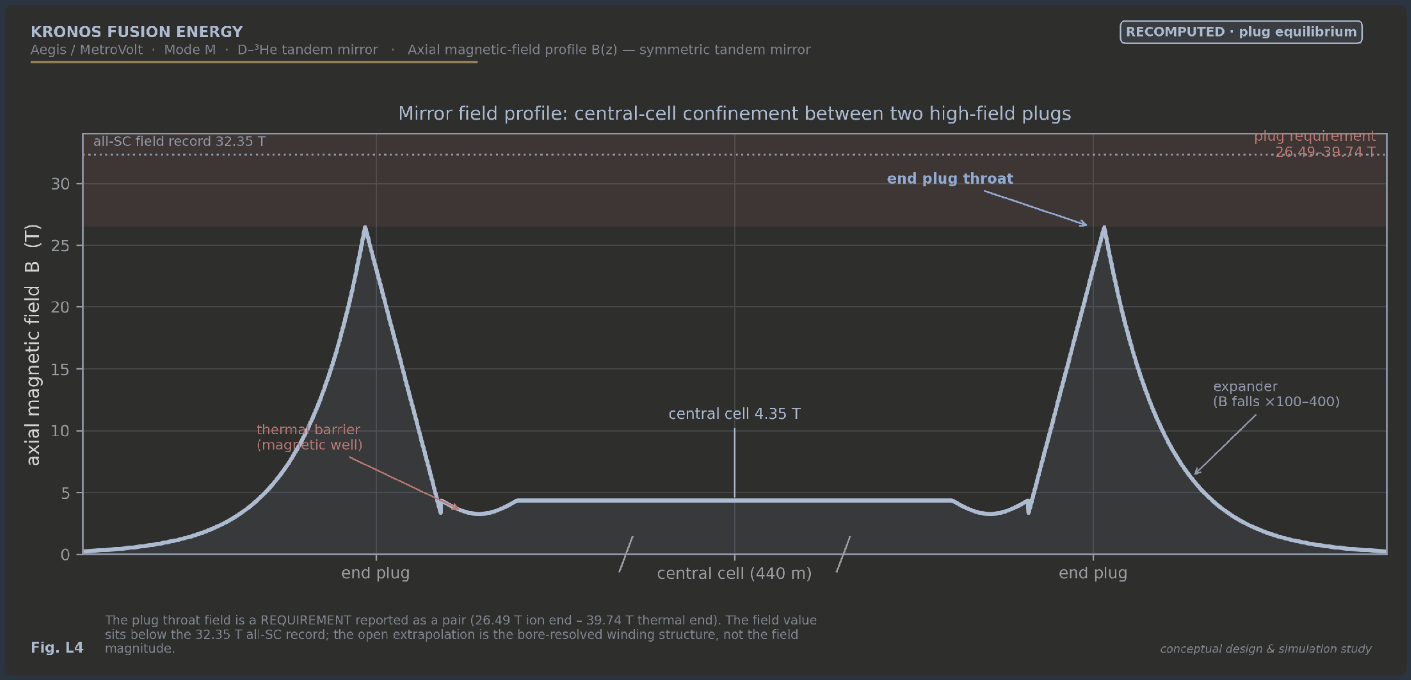

FIGURE 3. Axial magnetic field profile: a 4.35 T central cell rising to the 26.49–39.74 T plug throats, with the expander fields at the ends feeding the converters. RECOMPUTED

CONFIGURATION	**Axisymmetric high-field tandem mirror**, D–^{3}He fuel, end plugs, ions-only direct conversion (internal: Mode L / Mode M)
CENTRAL CELL	4.35 T solenoid · plasma minor radius a = 0.86 m · length is the free capital dial (55 / 440 / 1400 m)
PLUG THROAT	26.49 T (ion end) – 39.74 T (thermal end), reported as a pair from the Frank relation at $n_p/n_c \approx 16$
DESIGN OPERATING POINT	x(^{3}He) = 0.30 · T_i = 90 keV · $n_e = 2.6\times10^{20}$ m^{-3} · $n_p/n_c = 16$
RESULT	**Q_E = 1.31** · f_n = 5.44% *(low-neutron, not aneutronic)* · both intensive, length-independent

§ 5

Exhaust — axial extraction, no divertor, no ELMs

Because the field lines are open, exhaust leaves the machine *axially*, straight onto the direct-conversion collectors. There is no X-point, no separatrix, no strike point, and no edge pedestal to destabilise, so **edge-localised modes do not exist as a phenomenon** and no divertor is required. This is an architectural distinction from the tokamak breeder, not a mitigated version of the same problem. Triangularity is likewise undefined: an open system has no closed flux surfaces, so it is not a parameter this machine possesses — the companion breeder's δ declaration simply does not transfer.

The counterpart requirement is the end-collector heat flux, and it is stated as a requirement rather than claimed closed. At the reference point the axial loss delivers **906.2 MW** through the two end apertures, which is **195 MW m^{-2} unexpanded**. Flux conservation supplies the remedy: an end expander taking the field from the 26.49 T ion-end throat down to ≈ 0.5 T expands the collector area roughly **53**×, bringing the collector loading to **3.7 MW m^{-2}** — inside a divertor-class limit. No expander-field specification exists in the retrieved record, so this is a requirement-class item: the mirror's structural counterpart to the tokamak divertor problem, not an exemption from it.

REQUIREMENT

§ 6

Closure on measured component efficiencies

The device closes with positive engineering gain on measured efficiencies at the design operating point — *provided* the end plug reaches the required density ratio $n_p/n_c \approx 16$. Closure here means something specific and disciplined: ions-only conversion at $\eta_{ion} = 0.470$, the best measured tube, with *no requirement-class efficiency* anywhere in the balance and no near-ignition flag. At $x(^3He) = 0.30$ the result is **Q_E = 1.31**, for a net **+850 to +2832 MW_e** across the 440–1400 m configurations. The net scales with central-cell length; the gain and the neutron fraction f_n = 5.44% do not.

TABLE 1 · MODE M — THE REPRODUCIBLE CLOSING POINT (GAIN LENGTH-INDEPENDENT)

CENTRAL-CELL LENGTH	INTENSIVE POINT	P_{FUS}	NET ELECTRIC
55 m (reference)	Q_E 1.31 · f_n 5.44%	0.54 GW	+104 MW_e
440 m (Aegis)	— same intensive point —	4.3 GW	+850 MW_e
1400 m (MetroVolt)	— same intensive point —	13.7 GW	+2832 MW_e

MANDATORY CAVEAT — CLOSURE IS A REQUIREMENT, NOT A DEMONSTRATION

This closing point is **requirement-class**. It depends on an end-plug density ratio $n_p/n_c \approx 16$ — a plug density of $\approx 4 \times 10^{21}$ m^{-3}, roughly two orders of magnitude above any operated tandem-mirror plug and **347× the best value measured on GDT**. It is the design's single largest open item, specified rather than demonstrated. **At the reference ratio n_p/n_c = 10 the same balance does not close** — Q_E = 0.63, net negative. Every Q_E in this paper is quoted only with this requirement attached: an engineering target, not demonstrated physics. REQUIREMENT-CLASS

Two adjacent facts complete the picture, and both are more instructive than the headline. First, **pure deuterium does not close at any plug ratio**: Q_E falls to **0.42** (net −6.2 to −19.6 GW_e across the 440–1400 m configurations; −6197 MW_e at 440 m). Second — and this is the diagnostic point — the reason is a *charged-power budget*, not a confinement shortfall. At the design operating point (T_e = 90 keV) the charged power is a factor ≈ **5.8 short of the axial loss** (697 versus 4055 MW at 440 m), and that ratio is *length-independent*. Adding helium-3 lifts the charged fraction enough to close; nothing about confinement time can substitute for it. This is why closure in this machine is a helium-3 fraction, not a date.

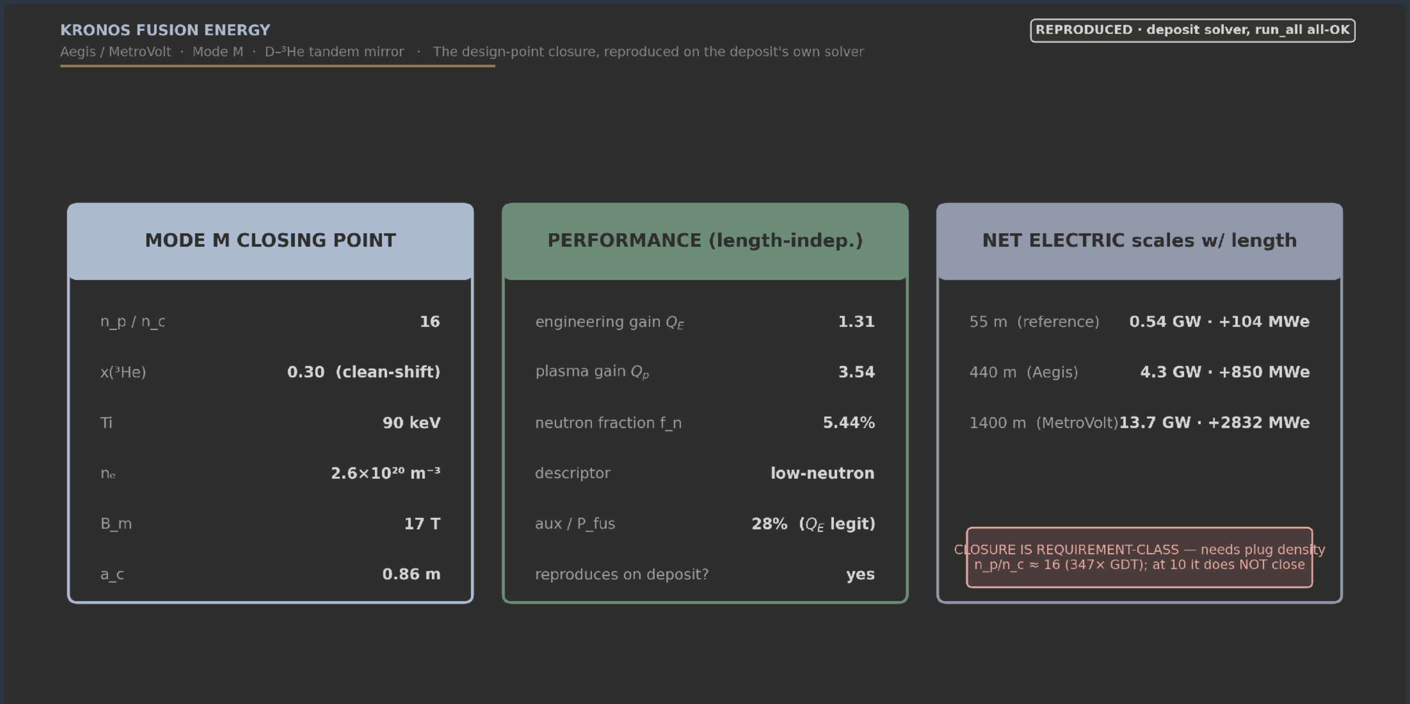

Fig. L8 The device closes at the design point on measured efficiencies: Q_E 1.31, net +850 to +2832 MWe across the 440-1400 m configurations. Q_E and f_n are length-independent; net electric scales with central-cell length. Closure is contingent on the end-plug density requirement (n_p/n_c ~ 16), the design's largest open item; at n_p/n_c = 10 it does not close.

FIGURE 4. The closure picture: the device closes at the design point ($x(^3He) = 0.30$, Q_E 1.31, net +850–2832 MW_e at the required $n_p/n_c \approx 16$), while pure deuterium fails (Q_E 0.42, net −6197 MW_e at 440 m) on the charged-power budget. RECOMPUTED · MODE M

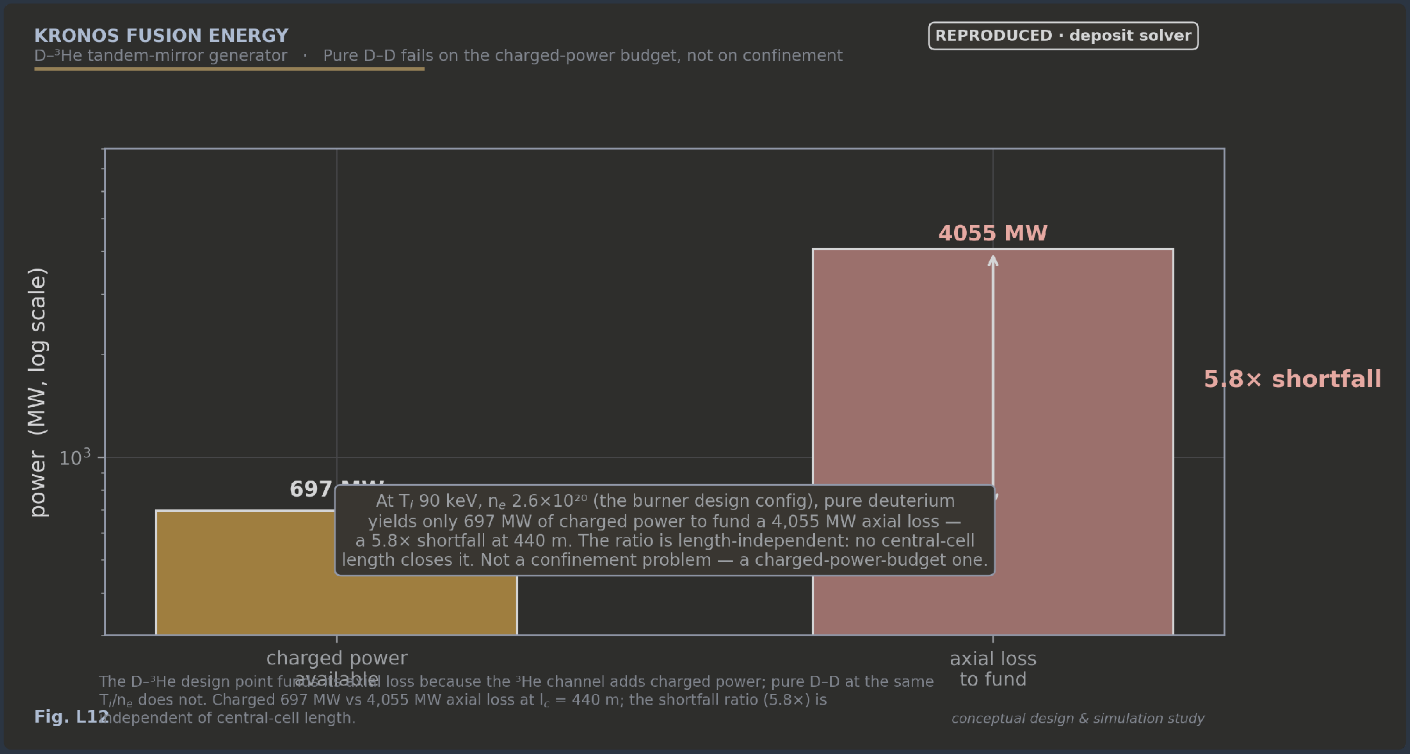

FIGURE 5. Why pure deuterium does not close: at the design point (T_e = 90 keV) the charged power is a factor 5.8 short of the axial loss (697 versus 4055 MW at 440 m; the ratio is length-independent). The mechanism is a charged-power budget, not confinement. Adding helium-3 lifts the charged fraction enough to close. DERIVED

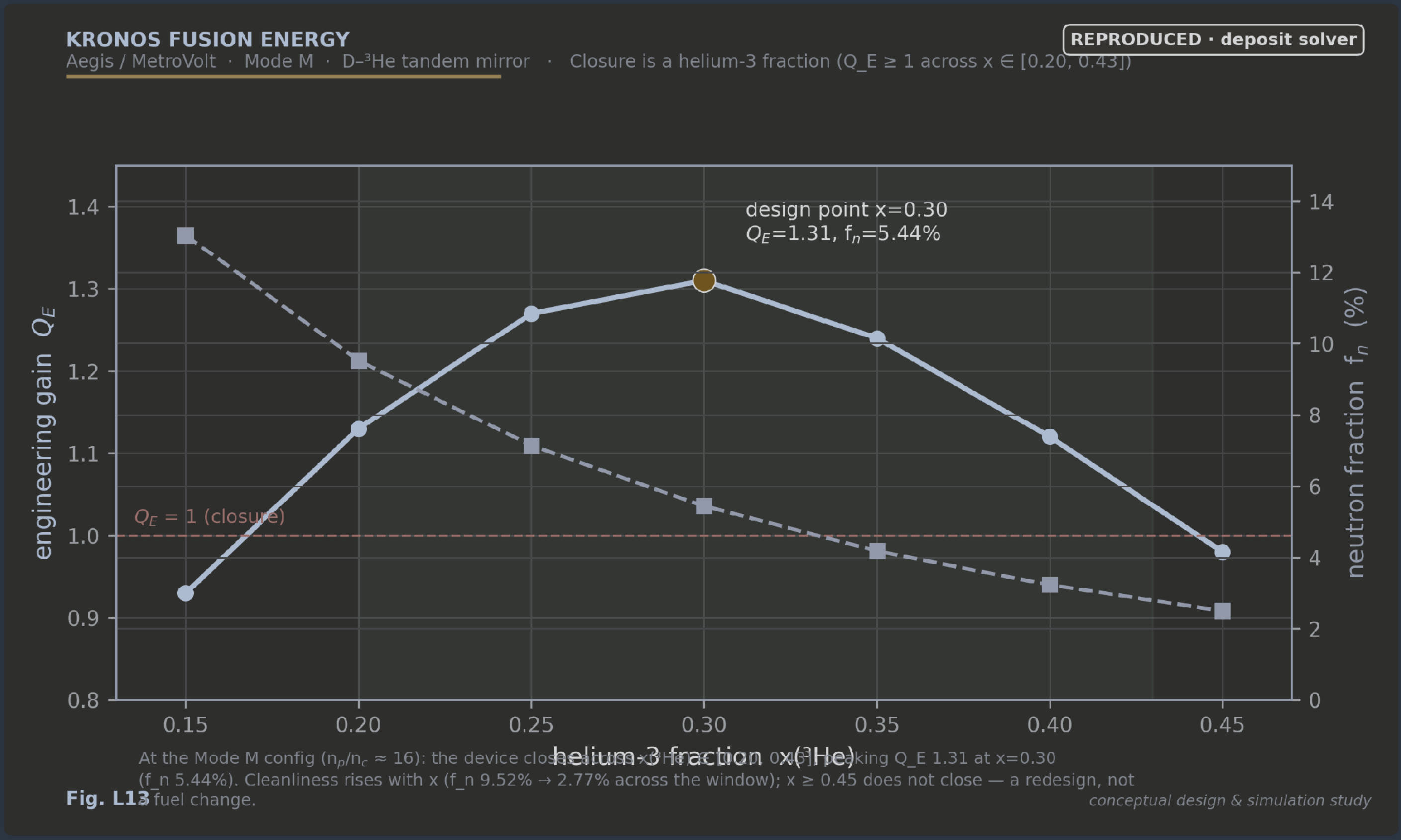

FIGURE 6. Closure is a helium-3 fraction, not a date. At the design point x(³He) = 0.30 the gain reaches Q_E 1.31 (at $n_p/n_c \approx 16$); pure deuterium (x = 0) fails at Q_E 0.42. Closure spans x(³He) ∈ [0.20, 0.43], with the neutron fraction falling 9.52% → 2.77%. DERIVED

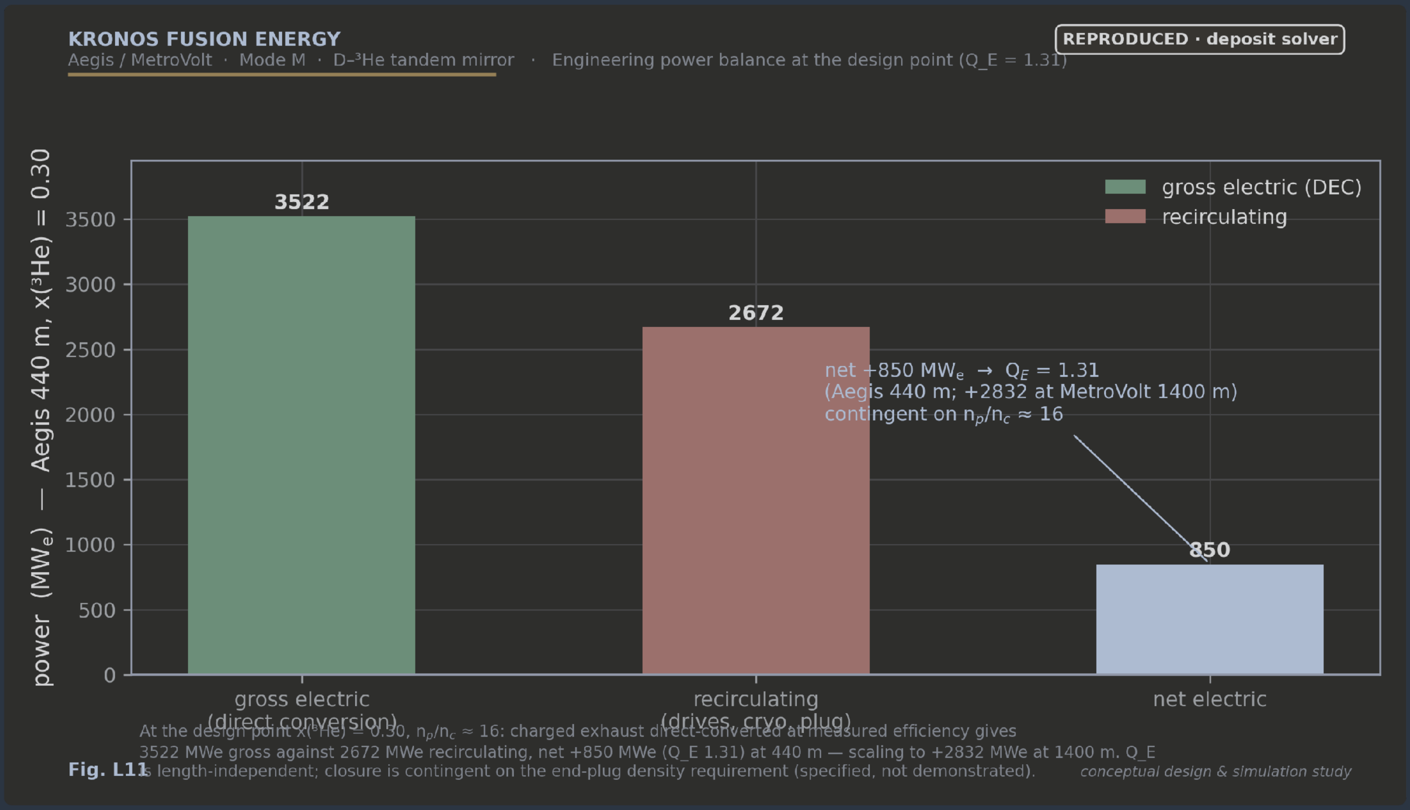

FIGURE 7. Engineering power balance at the design point ($x(^3He) = 0.30$, $n_p/n_c \approx 16$): gross direct-conversion electric exceeds the recirculating power to give $Q_E = 1.31$ and a net +850–2832 MW_e across the 440–1400 m configurations, on measured efficiencies — no requirement-class efficiency; the plug density is the requirement. DERIVED

Closure is a helium-3 fraction, not a date — and the gain is a floor obtained honestly, not a comfortable margin.

§ 7

The novel result — synchrotron loss is not a fixed fraction of fusion power

In a magnetised plasma the cyclotron harmonics below a cutoff are reabsorbed, and only the harmonics above it escape. The optical depth at harmonic n falls steeply with n — as n^{-3} in the relevant limit — while the escaping surface power at a given harmonic scales with the plasma surface-to-volume ratio, i.e. with 1/a. Setting the Rayleigh–Jeans surface ceiling equal to the optically-thin emission bound and solving for the harmonic at which they cross gives an *effective harmonic cutoff*

$$n^* \propto a^{1/3}\ n_e^{1/3}\ B^{-1/3} \tag{3}$$

with $n^* = 24.75$ at a = 0.86 m, $n_e = 10^{20}\ m^{-3}$, $T_e = 100$ keV and B = 5 T. Because the escaping power depends on which harmonics clear the cutoff, and n^* moves with the machine, **synchrotron loss is a function of device size, not a fixed fraction of fusion power**. A smaller device reabsorbs fewer harmonics and radiates more, at the same density and field. This is the one result in the program that rests *on* the geometry rather than despite it. DERIVED

The nearest prior treatment models reabsorption as a β-dependent scalar and cannot reproduce this size dependence; the closed-form synchrotron model of Albajar gives a loss but not a cutoff parameterisation. Two qualifications travel with the result and are stated in the same breath as the claim. It is a *reparameterisation*, not a measurement — the synchrotron uncertainty is reduced to one experimentally addressable parameter, not resolved — and any threshold quoted against n^* must state the engineering-gain convention it was computed on.

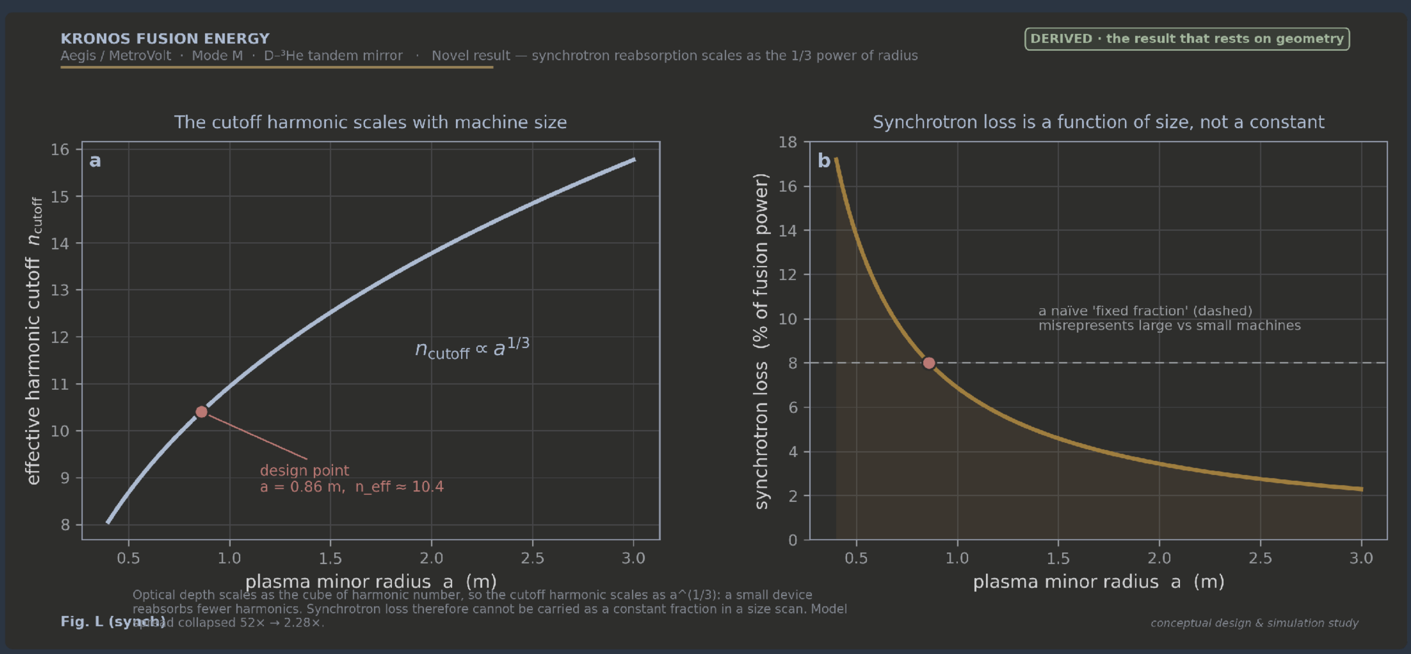

FIGURE 8. The synchrotron effective harmonic cutoff against plasma minor radius, $n^* \propto a^{1/3}$ (Eq. 3): synchrotron loss is a design lever, not a fixed fraction of fusion power. DERIVED

§ 8

Direct energy conversion — an honest ledger, not a blended efficiency

Direct conversion is applied to the *ion* stream only. The ion channel — the 14.66 MeV proton carrying the majority of D–^{3}He's charged output — is genuine direct energy conversion at measured tube efficiency. The electron/thermal channel is not, and crediting it at converter efficiency would be exactly the category error of the shared directability result: thermal energy converted to electricity is Carnot-bounded. This work therefore recovers the electron/thermal channel with a **bottoming cycle at 45–50%**, its documented default, not at converter efficiency. The penalty is stated plainly: the axial power split favours the electron stream, because the fast proton slows before reaching the converter, so splitting the channels honestly is *expensive rather than free*, and the resulting gain is a floor.

TABLE 2 · PER-STAGE DIRECT-CONVERSION EFFICIENCIES (EACH WITH ITS BASIS)

CHANNEL / STAGE	ADOPTED Η	BAND	BASIS
Ion collector (Venetian-blind class)	**0.470**	0.48–0.65	Best measured ion tube; flag: below the 0.60 two-stage optimum
Electron/thermal → bottoming cycle	0.45	–	Documented default; *not* converter efficiency
Thermionic topping on end-wall dump	0.505	0.45–0.56	Go *et al.* (2017), η_{TI} = 0.10 (TOPAZ-class)
Wall thermal + radiation, thermionic	0.10	0.10–0.20	TEC review; Carnot-consistent at 1000–1300 K
D–^{3}He spectrum	two discrete lines		p 14.66 MeV, α 3.69 MeV — favourable for grid-stack DEC
^{3}He–^{3}He spectrum	three-body continuum		**No transferable efficiency** — requirement

The exhaust train assumed here — cusp-type conversion for particle discrimination, followed by travelling-wave conversion for the high-energy protons, with the electron/thermal channel recovered by the bottoming cycle — is anticipated in full by two prior designs, one predating this work by a generation. It is presented as an implementation of established architecture, not as a contribution.

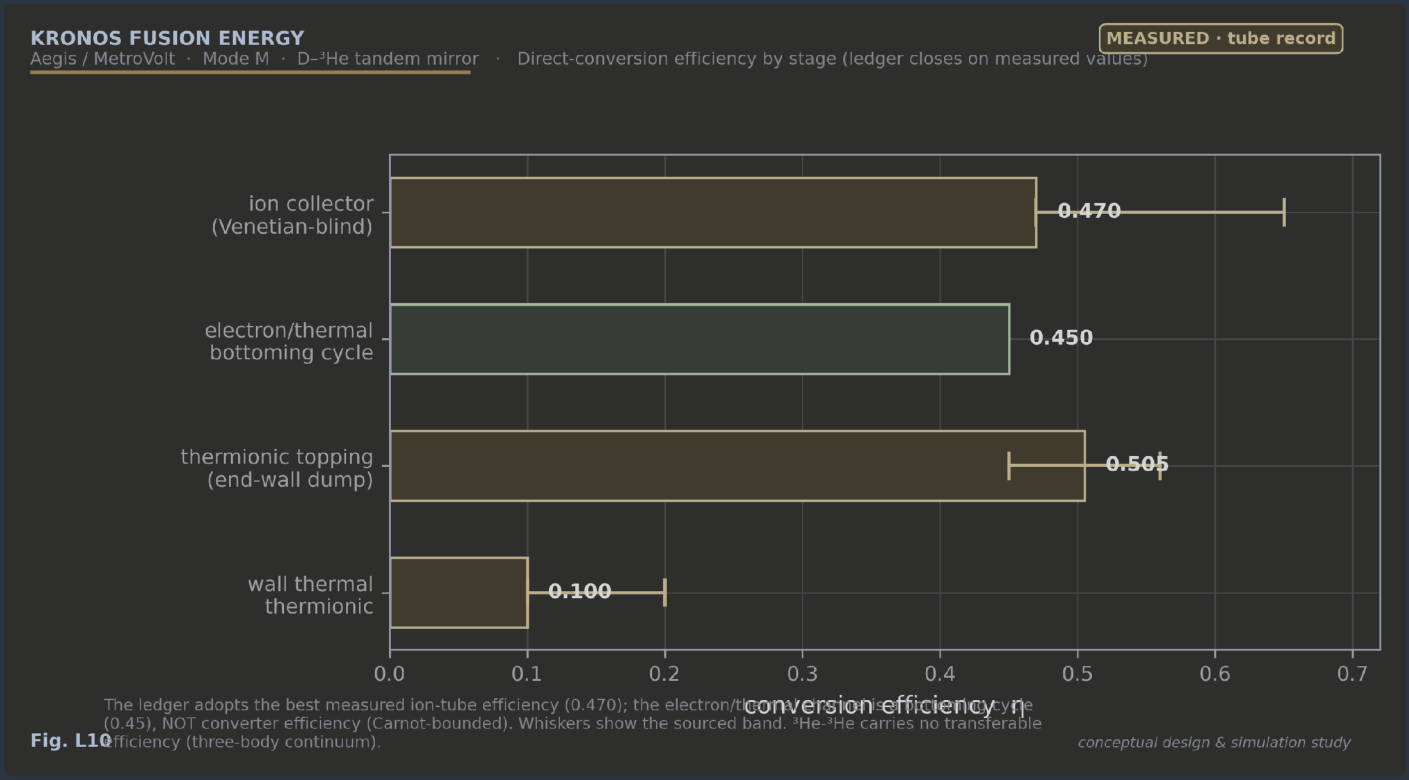

FIGURE 9. Direct-conversion efficiency by stage. The ledger closes on the best measured ion-tube efficiency (0.470); the electron/thermal channel is a bottoming cycle, not converter efficiency. Whiskers show the sourced band. MEASURED

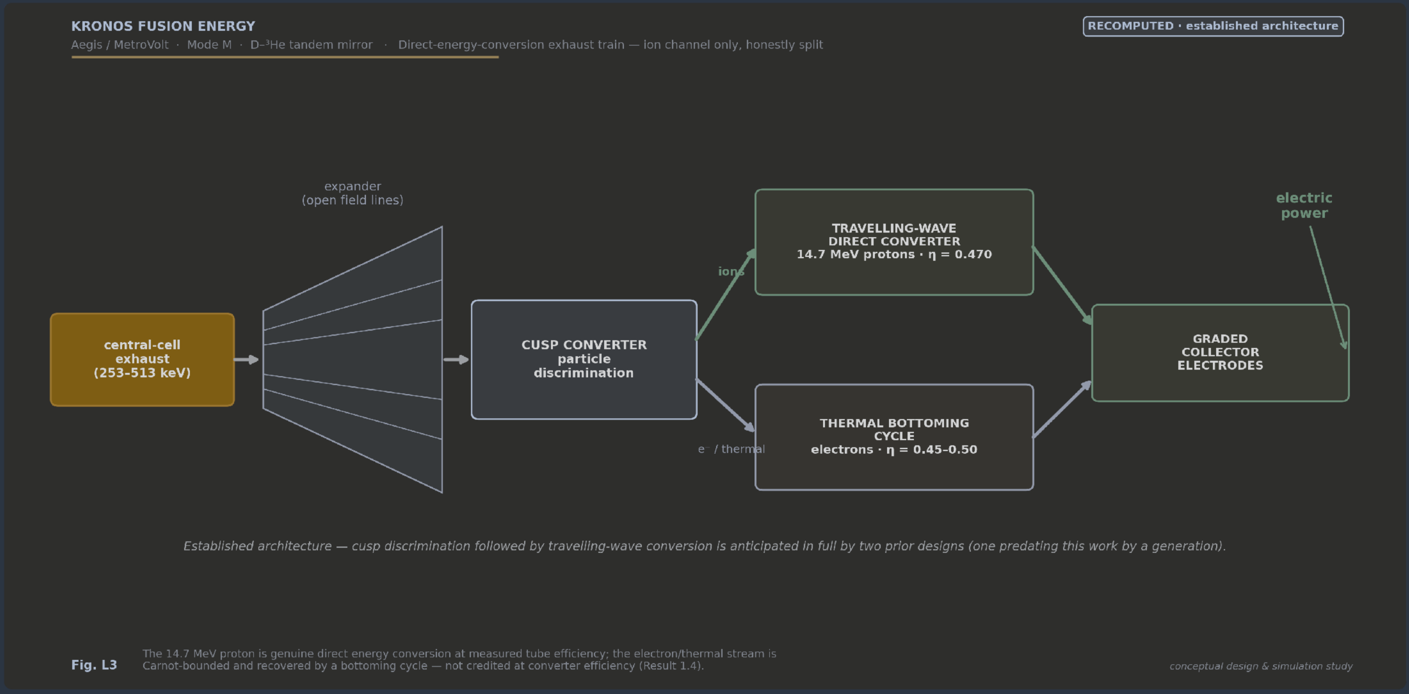

FIGURE 10. The direct-conversion exhaust train (implementation of established architecture): cusp-type particle discrimination, travelling-wave conversion of the high-energy protons, and electron/thermal recovery by a bottoming cycle. RECOMPUTED

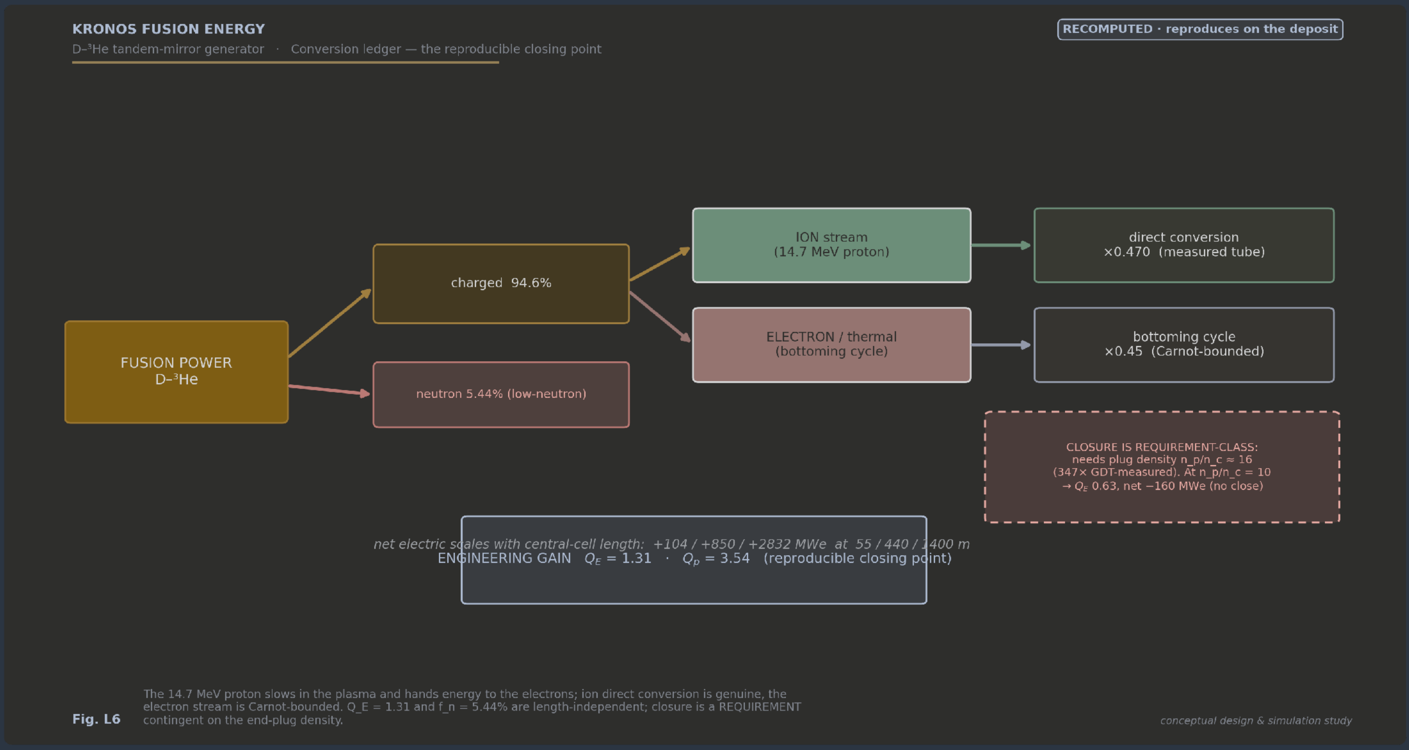

FIGURE 11. Per-channel conversion power ledger (megawatts). The axial split favours the electron stream, so splitting the channels honestly is expensive rather than free, and the resulting gain is a floor. RECOMPUTED

§ 9

Extrapolations — two, not three, plus one real gate

The generator's honesty is in its gates. The historical record for this class of machine carried three extrapolations forward as if equal; this work separates them by kind, and retires one outright. What remains is the plug *density* (the closure requirement of §6), electron direct conversion, and the thermal barrier — and only the last is a genuine physics gate.

THE PLUG FIELD IS NOT AN EXTRAPOLATION; THE PLUG COIL IS THE OPEN STRUCTURAL GATE

The plug throat field requirement is the pair **26.49–39.74 T**, which is **0.82**× an existing 32.35 T all-superconducting record. The field value sits below two existing REBCO magnets, so *the field is not the extrapolation*. The pure magnetic pressure at 26.49 T is **279 MPa**, and existing magnets operate above that in small bores. The honest location of the extrapolation is therefore the small-bore plug-coil *integration*: winding-pack geometry, current density, quench protection, and REBCO neutron lifetime at the residual (low-neutron, not zero) plug flux.

An earlier internal scaling that classified the field itself as an extrapolation is **withdrawn** as a method defect. The scaling $\sigma \propto (B/17)^2$ also declares the existing NHMFL 32 T and 45 T magnets unbuildable, because a field-squared form cannot see bore radius — whereas the hoop stress from the $J_\theta \times B_z$ body force scales as $\mathbf{J_\theta\, B_z\, r}$ (azimuthal current density, axial field, bore radius), and a small bore is the *favourable* direction. ~~WITHDRAWN · METHOD DEFECT~~

Yet even in that favourable direction, a structural analysis at the sourced design bore (a_1 = 0.648 m) finds the plug coil **infeasible**: peak hoop stress **2916–4253 MPa** (2.7–3.9× the reinforced allowable) at **4.6–6.5**× **the REBCO strain cap**. The plug winding is therefore carried as a requirement-class gate needing a strain-first architecture or a revised geometry — not an engineering refinement. As §10 shows, that gate is *resolved* by a stress-managed structural-shield architecture (scoping model, finite-element analysis pending), so the plug is carried as **feasible-pending-FEA** rather than closed. REQUIREMENT · RESOLVED PENDING FEA

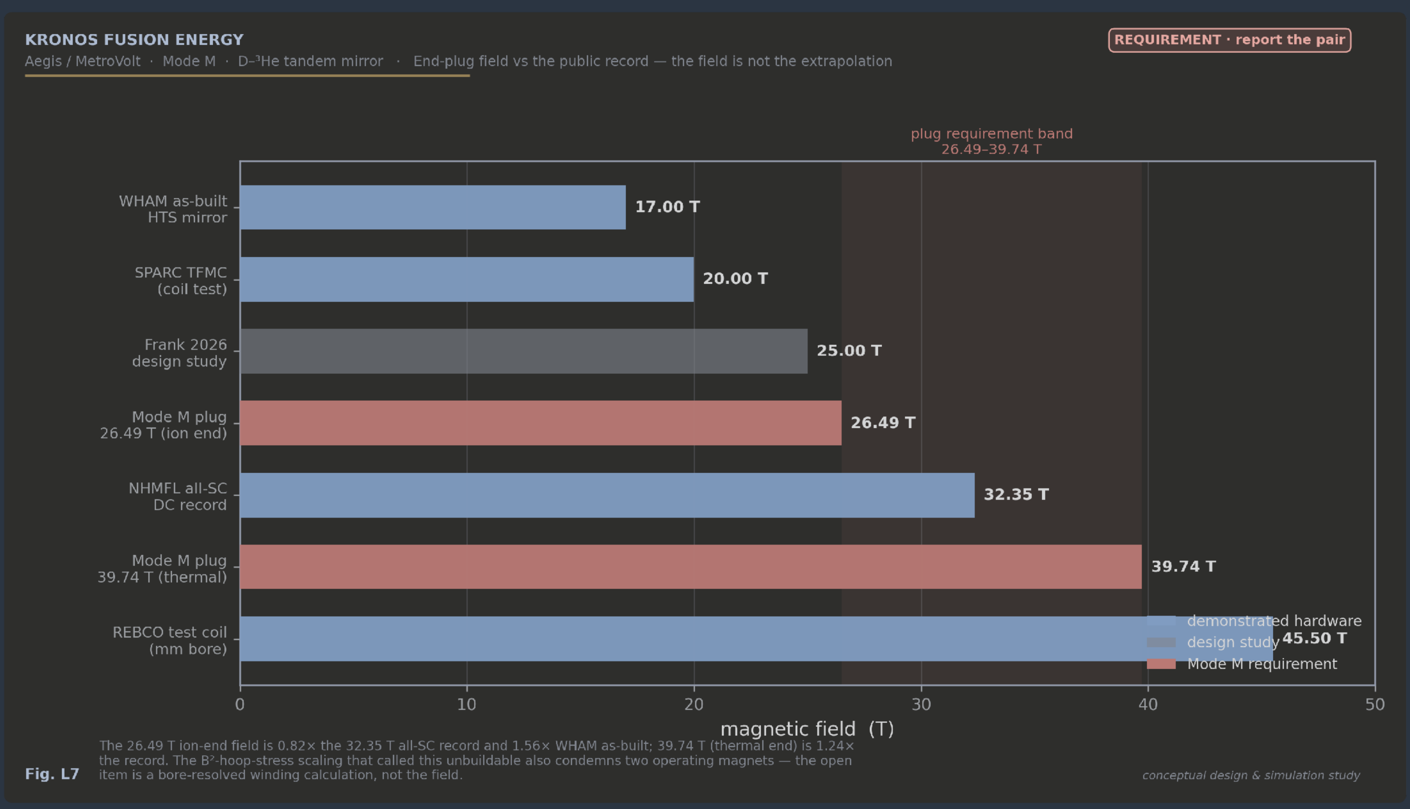

FIGURE 12. The plug-field requirement (26.49–39.74 T) against the public demonstrated record — WHAM (17 T), the SPARC TF model coil (20 T), and the 32.35 T all-superconducting record: the field is 0.82× an existing magnet. REQUIREMENT

ELECTRON DIRECT CONVERSION IS A REQUIREMENT; THE THERMAL BARRIER IS THE ONE REAL GATE

Electron direct conversion at the relevant energy appears *nowhere* in the retrieved experimental record and is stated as a requirement; every measured electrostatic result is on ion beams, and the ion-only closure of §6 does not use the electron channel at all. It is excluded from every closing number. REQUIREMENT

The **thermal barrier** was attempted on a historical tandem mirror and returned a *measured negative*. Re-analysis attributes the failure to programmatic rather than fundamental causes — the barrier was produced but not sustained under the diagnostics of the era — but a measured negative is a measured negative, and no stability actuator is named for this configuration. This is the one genuine remaining physics gate, honestly stated. REQUIREMENT · PHYSICS GATE

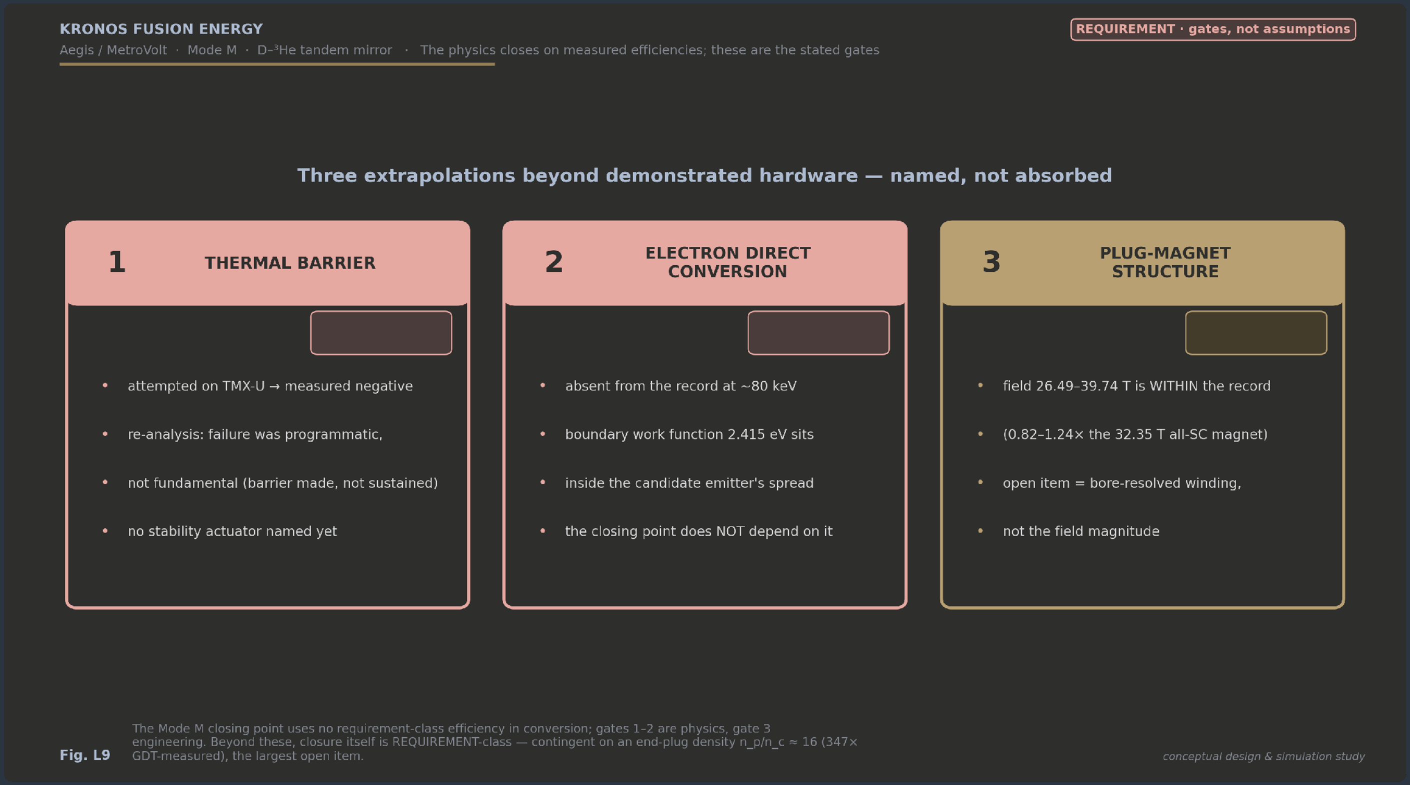

FIGURE 13. The named extrapolations and the one real physics gate (the thermal barrier), carried openly with their evidence class rather than absorbed into a single optimum — with the honest nuance that the plug *field* is within the demonstrated record while the plug *density* and electron direct conversion are named requirements. REQUIREMENT

§ 10

Enabling subsystems — the magnet and the control layer

RESOLVING THE PLUG-COIL GATE: A STRESS-MANAGED STRUCTURAL SHIELD

The requirement-class result of §9 is a *bare-winding bound* — the conservative case in which the winding carries its own hoop stress unaided. A companion magnet design study (in preparation; scoping model, finite-element analysis pending) finds the gate resolved, not fundamental, once three levers act together: (i) a low winding-pack current density, paid for in radial build; (ii) a mechanically segmented, pre-compressed winding rather than a bonded monolith; and (iii) making the neutron shield *structural* — a tungsten-based jacket serving simultaneously as shield, pre-compression shell and reinforcement — which shrinks the winding bore from 0.648 to ≈ 0.50 m and, because the hoop stress scales linearly with bore, cuts it proportionally.

TABLE 3 · REBCO PLUG-COIL FEASIBILITY TIERS AT THE 26.49 T THROAT FIELD

TIER	WINDING BORE	SHIELD	BUILD	STRAIN VS. CAP	BASIS
Bare winding (published bound)	0.648 m	30 cm passive	–	4.6–6.5× over	[D] infeasible
Stress-managed (reference)	0.50 m	15 cm structural	14 cm	0.4× (60% margin)	[T] design-study, FEA pending
Frontier (development target)	0.45 m	10 cm advanced	7 cm	0.4×	[R] not yet qualified

The realistic reference design closes at the full 26.49 T throat field with ≈ **60% strain margin** — a **1.74× magnetic-pressure extrapolation** over the demonstrated 20.1 T SPARC toroidal-field model coil. Its honest cost is that the compact structural shield passes more neutron flux, which favours a **demountable plug cartridge** — a maintenance cadence rather than a lifetime limit. The detailed mechanics are deferred to the companion; here the plug is carried as feasible-pending-FEA. REQUIREMENT · FEA PENDING

THE PLUG GATE, STATED IN ONE LINE

The plug *field* is within the demonstrated magnet record; the plug *coil* is infeasible as a bare winding but closes with ≈ 60% strain margin under a stress-managed structural shield, finite-element analysis pending. It is the burner's hardest open engineering gate — carried as feasible-pending-FEA, not a dead end. The plug *density* ($n_p/n_c \approx 16$), by contrast, remains the design's single largest open *physics* requirement.

CONTROL AND COMPUTATION

Real-time control of a nuclear-regulated generator is treated in a companion study (Zenodo 10.5281/zenodo.21842371): a layered digital-twin architecture in which physics-informed machine learning is deployable now inside a deterministically clamped safe set, quantum sensing is a near-term diagnostic tier, and quantum *computation* is an offline calibration tier with **no resource crossover this decade**. The closure and results of this paper do not depend on that layer; it is the certification and operations path, carried separately. NO CROSSOVER THIS DECADE

§ 11

Two housings — Aegis and MetroVolt, one physics result

Aegis and MetroVolt are the same tandem mirror at two central-cell lengths — the same intensive physics point, the same Q_E 1.31 and f_n 5.44%, differing only in the length that sets the net electric output. What separates them is the market they serve and the bar each must clear, not the physics inside them.

AEGIS	**Fixed defense installation power** — a 440 m central cell, 4.3 GW fusion, +850 MW_e net. Sold as resilient, fuel-logistics-free power for fixed sites; *not* naval, not propulsion, not transportable.
METROVOLT	**Data-center campus power** — a 1400 m central cell, 13.7 GW fusion, +2832 MW_e net. Last in the sequence: it must clear grid-competitive cost *and* lunar-scale helium-3 supply.
SHARED PHYSICS GATES	Closure requires the plug-density requirement ($n_p/n_c \approx 16$), the thermal barrier, and electron direct conversion — identical in both housings.
WASTE CHARACTER	**Low-neutron, not aneutronic** ($f_n \approx 5.44\%$) — stated as low, never zero.

Because the intensive point is length-independent, the central-cell length is the design's "free capital dial": the same closing physics is stretched from a 55 m reference demonstrator (+104 MW_e) to Aegis at 440 m and MetroVolt at 1400 m without touching Q_E or the neutron fraction. The mirror's open geometry — no divertor, no ELMs, no triangularity — is common to both, and so is the requirement-class end-expander that turns 906.2 MW of axial loss into a divertor-class 3.7 MW m^{-2} collector flux.

§ 12

Fuel cleanliness — a ramp, not a switch

The neutron fraction is a function of the helium-3 fraction, and the design point sits at a deliberate compromise rather than at the aneutronic limit. At $x(^3He) = 0.30$ the neutron fraction is 5.44%. Across the closure band $x(^3He) \in [0.20, 0.43]$ the neutron fraction falls from **9.52% to 2.77%** — cleaner fuel, but at a rising helium-3 demand and a narrowing power margin. Fuel cleanliness is therefore a ramp the operator climbs as helium-3 supply allows, not a switch that is thrown once.

HELIUM-3 FRACTION $X(^3HE)$	NEUTRON FRACTION F_N	STATUS
0.20 (clean-fuel edge of closure)	9.52%	Closes ($Q_E > 1$ at $n_p/n_c \approx 16$)
0.30 (design operating point)	**5.44%**	**Q_E 1.31 — the frozen point**
0.43 (upper edge of closure)	2.77%	Closes; cleanest fuel in band

The honest framing bears repeating: the machine is **low-neutron, never aneutronic**. Even at the cleanest end of the closure band the fuel produces a residual neutron flux, and every waste, activation and magnet-lifetime statement in this program is written against that residual, not against zero. The plug coil's REBCO neutron lifetime (§9–§10) is a direct consequence.

§ 13

Comparison with prior mirror and D–^{3}He designs

The mirror concept and the converter architecture are prior art. What is distinctive here is the discipline applied to them: closing on measured efficiencies, the size-dependent synchrotron result, and the explicit gate accounting with a stated fail branch.

TABLE 4 · THIS WORK AGAINST THE PRIOR DESIGN LINEAGE

AXIS	PRIOR DESIGNS (RA, ARTEMIS, WHAM)	THIS WORK
Converter efficiency basis	Aspirational (≈ 70–80% projected)	Measured ion-tube (0.470), flagged
Synchrotron treatment	Fixed fraction / β-scalar	Size-dependent cutoff $n^* \propto a^{1/3}$
Plug field	— (WHAM as-built 17 T)	26.49 T, stated as 0.82× an existing record
Extrapolations	Often absorbed into one optimum	Two named + one physics gate, with a fail branch

§ 14

Discussion — why the physics is reported without economics

The generator's physics stands on its own and is deliberately reported without economics. Its near-term value is a physics result and a technology base — high-field magnets and direct conversion — and any commercial analysis is confined to a separate companion. The honest posture is threefold: closure rests on measured efficiencies with one recovered deficit stated as a requirement; synchrotron loss is now a design lever rather than a fixed uncertainty; and of the three historical extrapolations, only the thermal barrier remains a genuine physics gate.

That is a materially stronger and more truthful position than a single blended optimum — and it is precisely why the generator paper is separated from, and not contingent on, the breeder economics. A reader who wants to attack the result can find the load-bearing assumption in one line (the plug density), rather than having to reverse-engineer it out of an averaged converter efficiency.

§ 15

Limitations — the open items, in one place

The limitations are stated together so that no reader has to assemble them from the body. Each is an open item, and each is named with its evidence class.

- **The end-plug density is the largest open item.** $Q_E = 1.31$ is computed on measured efficiencies but is *contingent* on $n_p/n_c \approx 16$ — specified, not demonstrated, and 347× the GDT-measured plug. At the reference ratio the balance does not close ($Q_E = 0.63$). REQUIREMENT

The thermal barrier is the one physics gate, with a measured historical negative and no named stability actuator. PHYSICS GATE

Electron direct conversion is a requirement — absent from the retrieved experimental record at the relevant energy, and excluded from every closing number. REQUIREMENT

The plug coil is feasible-pending-FEA, not closed: infeasible as a bare winding, resolved by a stress-managed structural shield with ≈ 60% strain margin, finite-element analysis pending. FEA PENDING

The end-expander field has no specification in the record; the 906.2 MW → 3.7 MW m^{-2} collector remedy is stated as a requirement, not a closure. REQUIREMENT

Pure-D–D non-closure is a charged-power-budget result (a factor 5.8 short), and it is structural across T_e 90–400 keV — not fixable by confinement. DERIVED

^{3}He–^{3}He carries no transferable conversion efficiency from D–^{3}He; the two fuels are not interchangeable in the ledger. DEFINITIONAL

Wall reflectivity has no measurement at the relevant frequencies; the synchrotron budget is carried by margin, not by measured optical constants. UNMEASURED

The assumed capacity factor is unsupported (no component-lifetime basis) and is used in no physics claim here. UNSUPPORTED

§ 16

Conclusion

A deuterium–helium-3 tandem-mirror generator closes with positive engineering gain on *measured* component efficiencies at the design operating point ($x(^3He) = 0.30$): $\mathbf{Q_E = 1.31}$, for a net electric output of **+850 to +2832 $\mathbf{MW_e}$** across the 440–1400 m configurations, with no requirement-class *efficiency* in the balance. That closure is contingent on a single named requirement — an end-plug density ratio $n_p/n_c \approx 16$, specified but not demonstrated and the design's largest open item. At the reference plug ratio the balance does not close ($Q_E = 0.63$), and pure deuterium does not close at any plug ratio ($Q_E = 0.42$) — for a charged-power-budget reason rather than a confinement one.

The study's principal new result is that synchrotron reabsorption is size-dependent — the effective harmonic cutoff scales as $n^* \propto a^{1/3}$ — so synchrotron loss is a design lever rather than a fixed fraction of fusion power. Of the three historical extrapolations, the plug *field* is retired (0.82× an existing all-superconducting record), leaving the plug *density* and electron direct conversion as named requirements and the thermal barrier — which returned a measured negative on a historical tandem mirror — as the one genuine physics gate. The fuel is low-neutron, never aneutronic ($f_n = 5.44\%$ at the design point). The physics stands on its own and is reported without economics, which are treated separately and are not a condition of the result.

> **THE ONE-LINE SUMMARY A DILIGENCE READER CAN HOLD**
>
> The generator closes at Q_E 1.31 on measured efficiencies — but only if an end-plug density 347× the best ever measured can be reached. That single requirement, not the magnet field and not the converter, is the machine's make-or-break physics gate, and it is stated first, never hidden. The synchrotron result is the paper's genuine contribution; the thermal barrier is its one honest physics unknown.

APPARATUS

Portfolio, People & Record

The intellectual-property estate, the people who built it, the limitations that gate it, and the sources it rests on.

1	4	40	27
GRANTED PATENT	2026 PROVISIONALS	TEAM MEMBERS	2022 PROVISIONALS

INTELLECTUAL PROPERTY

The patent portfolio

The estate spans a granted high-field magnet patent, pending utility and 2026 provisional filings that map to the two products, a digital-twin control provisional, a registered trademark application, and the original 2022 provisional family. Every patentable disclosure in the five-paper arXiv drop was protected **before** publication: the breeder and burner provisionals were filed 1–2 August, and a publication-gap omnibus filing the evening before the drop swept up the DEC, plasma-control, and REBCO-winding matter of the three otherwise-unprotected papers. Patent numbers and application serials are matters of public record; claim scope is summarised, not reproduced.

GRANTED & PENDING UTILITY

US 12,009,112	High-field tilted graded-REBCO magnet architecture (KRONO-002A) · *app. 17/878,550*	GRANTED
US 17/878,507	Core device / method (KRONO-001A) · *utility*	PENDING

2026 PROVISIONAL FILINGS — MAPPED TO THE PRODUCTS

64/124,209	Hyperion — spherical-tokamak tritium / helium-3 foundry · *breeder · filed Aug 2026*	FILED
64/124,220	Aegis / MetroVolt — synchrotron-cutoff, fuel-selection & plug-winding · *generator · filed Aug 2026*	FILED
64/115,167	KRONOS-CTRL digital-twin plant control · *provisional · filed Jul 2026*	FILED
64/005,440	Integrated spherical-tokamak fusion architecture · *early integrated-architecture filing · filed Mar 2026*	FILED
64/105,530	Negative-triangularity spherical-tokamak architecture · *foundational ST filing · filed Jul 2026*	FILED
64/128,097	Publication-gap omnibus — quasineutral two-species expander DEC · provenance-gated / latency-split plasma control · as-built high-field winding & conductor architecture · *filed 7 Aug 2026, the evening before the arXiv drop*	FILED

TRADEMARK & ORIGIN

FTK-98801894	Kronos Fusion Energy — trademark application	FILED
KR-2022-*	Original provisional family (KR-2022-00001 … 00027) · *27 filings, 2022*	PRIORITY

The narrow, defensible magnet novelty — the specific conductor and the digital-twin winding optimisation, not high-field REBCO as a category — is the commercial core that can earn ahead of any Q > 1 milestone, with markets in fusion magnet supply, MRI/NMR, accelerators, and proton therapy. The claim is scoped honestly: the high field is a *system field* result, not a stand-alone-coil record; the small-bore plug coil is structurally infeasible as a bare winding but resolved by a stress-managed structural shield (feasible-pending-FEA); and the winding-tape experiment returned a *null result*. The value is the method, not a field record.

THE TEAM

Founding partners, board, advisors & auditors

Kronos is built by a bench of advanced-fuel-fusion, high-field-magnet, direct-conversion, and materials specialists, with a board and operations team drawn from defense, national laboratories, and industry. Dates are shown as ranges; where a tenure has ended or is term-ending, the range says so.

FOUNDING PARTNERS — SCIENCE

Dr. Gerald Kulcinski
Co-Founder · Helium-3 & Advanced-Fuel Fusion
UW–Madison · 2023–Present

Dr. Carl Weggel
Chief Scientist / S.M.A.R.T. Design
MIT Alcator Program · 2022–Present

Dr. Robert J. Weggel
Magnetic Field Design
MIT Magnet Lab · 2022–Present

BOARD

Priyanca Ford
Founder & CEO · Executive Board
2022–Present

Bandel Carano
Finance / Strategy
Oak Investment Partners / Stanford · 2025–2026

Patrick Schweiger
Fusion Device Engineering
Oklo / CFS / TerraPower · 2025–Present

SCIENTIFIC ADVISORS

Dr. Steven O. Dean
Fusion Policy & History
DOE / Fusion Power Associates · 2025–Present

Dr. Patrick H. Diamond
Plasma Turbulence & Transport
UC San Diego · 2025–Present

Dr. Jack J. Dongarra
HPC & Numerical Algorithms
Turing Award · 2025–Present

Dr. Nasr M. Ghoniem
Chief Material Scientist
UCLA · 2025–Present

Dr. Siegfried Glenzer
Plasma Physics & Laser Fusion
Stanford / SLAC · 2022–Present

Dr. David A. Hammer
Pulsed-Power Fusion
Cornell · 2025–Present

Dr. Donald A. Spong
Plasma Theory & Confinement
ORNL · 2025–Present

Dr. Curtis Smith
Risk Assessment & Nuclear PRA
MIT / Idaho National Lab · 2025–Present

RADM (Ret.) David Goggins
Naval Engineering & Power-Plant Design
U.S. Navy · 2023–2026

Dr. Konstantin Batygin
Mathematician
Caltech · 2022–2025

Dr. Ruben Fair
Magnet Design / ITER Liaison
PPPL / Jefferson Lab · 2022–2025

Dr. Paul S. Weiss
Materials & Nanotechnology
UCLA · 2022–2025

SCIENTIFIC AUDITORS

Dr. Wilfred A. Cooper
Plasma Equilibrium Theory
EPFL / Swiss Plasma Center · 2025–Present

Dr. Ahmed Hassanein
Plasma–Material Interactions
Purdue / Argonne · 2025–Present

Dr. Patrick E. Hopkins
Extreme Thermal Materials
U. of Virginia · 2025–Present

Dr. Peter Hosemann
Materials Joining & Structural Integrity
UC Berkeley · 2025–Present

Dr. Travis W. Knight
Advanced Nuclear Fuels & Systems
U. of South Carolina · 2025–Present

Dr. Philippe Lebrun
Cryogenics & Magnet Cooling
CERN · 2025–Present

Dr. Nitendra Singh
Nuclear Safety & Fuel Cycle
ITER · 2025–Present

Dr. Guido Van Oost
Magnetic Confinement & Fusion Systems
Ghent University · 2025–Present

Dr. Gary S. Was
Radiation Materials & Structural Integrity
U. of Michigan · 2025–Present

Dr. Ray Sedwick
Direct Energy Conversion
U. of Maryland · 2025

OPERATIONS

Michael Laughlin
Chief Operating Officer
2022–Present

Martin Owens
Chief Strategy Officer
LANL / GE Hitachi · 2022–Present

MG (Ret.) Paul Pardew
Chief Contracting Officer
Army Contracting Command · 2022–Present

David Beck
Fusion Commercialization
U.S. Space Force · 2024–Present

Sushma Bhatia
Environmental & Legislative
Google · 2022–Present

Michael De Frenza
Technology Licensing
2023–Present

MG (Ret.) Robin L. Fontes
Cybersecurity & Defense
Army Cyber Command · 2022–Present

Vijay Gehani
Supply Chain & Components
INOX India · 2024–Present

Jon Michel Greenwood
IT & AI Infrastructure
Live Nation · 2023–Present

Brian C. O'Neill
National Security
CIA / ODNI · 2022–Present

Gen. (Ret.) Gustave F. Perna
DoD Liaison
Operation Warp Speed · 2022–2023

Andrea Romero
Marketing Lead
2022–Present

Legal counsel is retained; those roles are held on the internal roster and are not listed here.

LIST OF FIGURES

List of Figures

LIST OF TABLES

List of Tables

REFERENCES

Sources

[1] H.-S. Bosch and G. M. Hale, “Improved formulas for fusion cross-sections and thermal reactivities,” *Nuclear Fusion* **32**, 611 (1992).

[2] A. S. Richardson, *NRL Plasma Formulary*, Naval Research Laboratory (2019).

[3] I. E. Ochs, E. J. Kolmes, and N. J. Fisch, “Bremsstrahlung and the electron–electron contribution in fusion plasmas,” *Physics of Plasmas* (2024).

[4] T. H. Rider, “Fundamental limitations on plasma fusion systems not in thermodynamic equilibrium,” *Physics of Plasmas* **4**, 1039 (1997).

[5] ITER Physics Expert Groups, “ITER Physics Basis,” *Nuclear Fusion* **39**, 2137 (1999).

[6] N. A. Uckan and J. Sheffield, “Tokamak scaling and confinement,” in *Tokamak Concept Improvement*, IAEA (1989).

[7] O. Sauter, C. Angioni, and Y. R. Lin-Liu, “Neoclassical conductivity and bootstrap current,” *Physics of Plasmas* **6**, 2834 (1999).

[8] F. Troyon *et al.*, “MHD limits to plasma confinement,” *Plasma Physics and Controlled Fusion* **26**, 209 (1984).

[9] J. P. Freidberg, *Plasma Physics and Fusion Energy*, Cambridge University Press (2007).

[10] R. F. Post, “The magnetic mirror approach to fusion,” *Nuclear Fusion* **27**, 1579 (1987).

[11] D. E. Baldwin, “End-loss processes from mirror machines,” *Reviews of Modern Physics* **49**, 317 (1977).

[12] T. K. Fowler, R. W. Moir, and T. C. Simonen, “A new simpler tandem mirror,” *Nuclear Fusion* **57**, 056014 (2017).

[13] G. L. Kulcinski and J. F. Santarius, “Advanced fuels and the D–^{3}He cycle,” University of Wisconsin Fusion Technology Institute.

[14] W. L. Barr and R. W. Moir, “Test results on direct energy converters for mirror reactors,” *Nuclear Technology/Fusion* **3**, 98 (1983).

[15] D. B. Go *et al.*, “Thermionic energy conversion in the twenty-first century,” *Frontiers in Mechanical Engineering* **3**, 13 (2017).

[16] M. Wang *et al.*, “The AME 2020 atomic mass evaluation,” *Chinese Physics C* **45**, 030003 (2021).

[17] J. E. Menard *et al.*, “Fusion nuclear science facilities and pilot plants based on the spherical tokamak,” *Nuclear Fusion* **56**, 106023 (2016).

[18] A. J. Creely *et al.*, “Overview of the SPARC tokamak,” *Journal of Plasma Physics* **86**, 865860502 (2020).

[19] T. P. Wright, “Factors affecting the cost of airplanes,” *Journal of the Aeronautical Sciences* **3**, 122 (1936).

[20] U.S. Department of Energy / NNSA, *Stockpile Stewardship and Management Plan*, FY2024.

[21] J. F. Santarius, G. L. Kulcinski, and L. A. El-Guebaly, “A strategy for D–^{3}He fusion energy development,” *Journal of Fusion Energy* **17**, 33 (1998).

[22] M. A. Abdou *et al.*, APEX advanced blanket concepts, *Fusion Engineering and Design* (1999–2003).

[23] Federal Register, notice on supply of tritium to non-federal entities (1999).

[24] Kronos Fusion Energy, “Simulation register and reproducibility deposit,” Zenodo (2026).

[25] A. O. Thome *et al.*, “ELM-free negative-triangularity edge on DIII-D,” *Plasma Physics and Controlled Fusion* (2024), doi:10.1088/1361-6587/ad6f40.

[26] T. Eich *et al.*, “Scaling of the tokamak near scrape-off layer power width,” *Nuclear Fusion* **53**, 093031 (2013).

[27] J. Lim *et al.*, “Scrape-off-layer width in negative-triangularity plasmas,” *Nuclear Fusion / Plasma Physics and Controlled Fusion* (2023).

[28] A. O. Nelson *et al.*, "Prohibition of second-stability access at negative triangularity," *Plasma Physics and Controlled Fusion* **64**, 124002 (2022).

COLOPHON

How this document was made

The Kronos Fleet — Combined Editorial, 2026 is set in **Fraunces** (display), **Gelasio** (text), and **IBM Plex Mono** (data & equations), carried forward from the Kronos editorial design system.

The figures are rendered at 300 dpi from the deposited generator scripts; the document is composed as a single self-contained file with embedded fonts and imagery, paginated to US Letter, and rendered to PDF through a headless Chromium engine in matched light and dark editions.

Every headline quantity carries an evidence class; withdrawn and restated values are marked as such. Nothing herein is frozen beyond the founder-approved Tier-A set.

Explore it live — turn the interactive 3-D model, run the deposited solvers in the physics validator, and watch the companion film series.

LEGAL NOTICE

Notice, status, and distribution

Conceptual design & simulation study. This document reports a conceptual design and simulation study. It is not a construction commitment, a safety-analysis report, a regulatory filing, or an offer of securities. Forward-looking statements — schedules, costs, market sizes, and performance — are estimates subject to the limitations set out in the Simulations part and may change.

Numbers and their classes. Quantities are reported with evidence classes and case labels; modelled, assumed, and requirement-class values are identified as such and are not to be quoted without their labels.

Public edition. This edition carries the physics and design only; all financial, funding, and defense-commercial content has been removed for public distribution. The scientific text corresponds to the arXiv and journal submissions.

THE 2026 KRONOS SET

One programme, in five papers

This editorial is one of five that together describe the Kronos fusion programme — a breeder that funds a generator, and the magnet, conversion, and control science that enable both. Each is published open-access with a reproducible companion deposit.

PAPER I	**Hyperion — The Tritium Foundry** · 10.5281/zenodo.21746157
PAPER II	**Aegis & MetroVolt — The Generator** *(this paper)* · 10.5281/zenodo.21746479
PAPER III	**High-Field REBCO Magnets & Tape** · 10.5281/zenodo.21842514
PAPER IV	**Direct Energy Conversion** · 10.5281/zenodo.21842864
PAPER V	**AI, ML & Quantum Control** · 10.5281/zenodo.21842371

Explore the whole programme live: the interactive 3-D model, the in-browser physics validator, and the companion film series.

KRONOS FUSION ENERGY

Aegis & MetroVolt

Explore the science — live, in your browser.

kronosfusionenergy.com/3D-Model

kronosfusionenergy.com/physics-Validation-Simulation

Companion film series · YouTube

Zenodo · DOI 10.5281/zenodo.21746479